Planetary Ions Acceleration in a Hot Flow Anomaly at Mars

Artyom Shestakov[1] and Sergey Shuvalov[2]

[1]Space research institute, Moscow
[2]Space Research Institute, Moscow, Russia

June 14, 2023

Abstract

Previous observation of a single hot flow anomaly (HFA) at Earth by MMS mission reported solar wind protons effective acceleration inside these structures to nearly 1 MeV under certain conditions via first-order Fermi acceleration process. Current study focuses on the analysis of a single HFA registered at Mars by MAVEN spacecraft. The event is characterized by the presence of accelerated O+ and O2+ ions of planetary origin on both sides from the current sheet associated with the event. Ions with energies up to ˜10 keV are detected before the current sheet crossing, and over 30 keV after the current sheet crossing. We report that the relationship between the ion mass and the maximum energy to which acceleration occurs is consistent with the above-mentioned Fermi acceleration process. We hypothetize that effective planetary ions acceleration in HFAs is possible only at unmagnetized planets due to closer bow shock stand-off distance.

Hosted file

`964225_0_art_file_11020648_rv5yd8.docx` available at https://authorea.com/users/625988/articles/647636-planetary-ions-acceleration-in-a-hot-flow-anomaly-at-mars

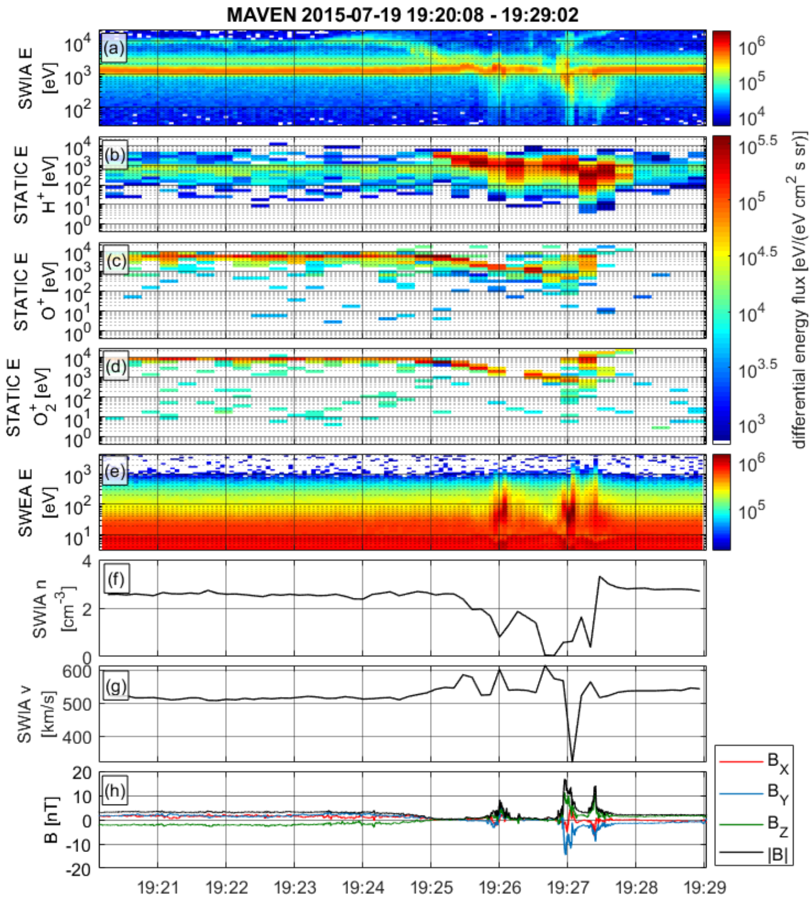
MAVEN 2015-07-19 19:20:08 - 19:29:02
SWIA E [eV]
STATIC E H+ [eV]
STATIC E O+ [eV]
STATIC E O2+ [eV]
SWEA E [eV]
SWIA n [cm-3]
SWIA v [km/s]
B [nT]
differential energy flux [eV/(eV cm2 s sr)]
(a)
(b)
(c)
(d)
(e)
(f)
(g)
(h)
BX
BY
BZ
|B|
19:21
19:22
19:23
19:24
19:25
19:26
19:27
19:28
19:29

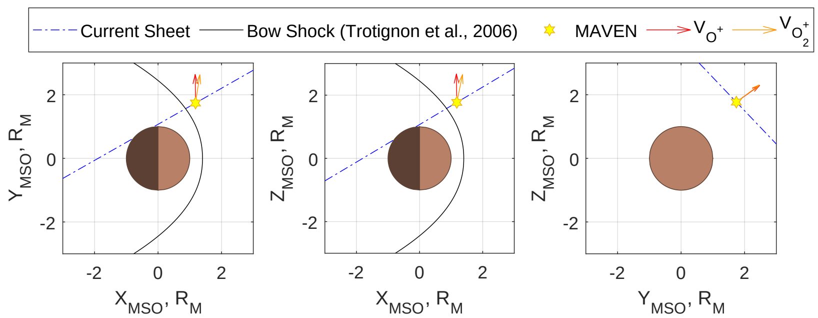

Current Sheet
Bow Shock (Trotignon et al., 2006)
MAVEN
V_{O^+}
$V_{O_2^+}$
Y_{MSO}, R_M
X_{MSO}, R_M
Z_{MSO}, R_M
X_{MSO}, R_M
Z_{MSO}, R_M
Y_{MSO}, R_M

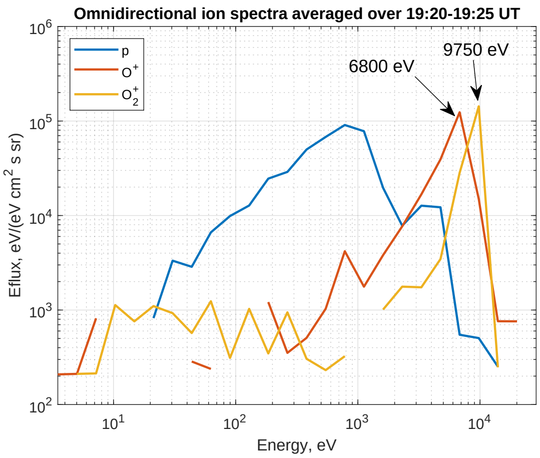
Omnidirectional ion spectra averaged over 19:20-19:25 UT
p
O+
O2+
6800 eV
9750 eV
Eflux, eV/(eV cm2 s sr)
Energy, eV
10^2
10^3
10^4
10^5
10^6
10^1
10^2
10^3
10^4

Planetary Ions Acceleration in a Hot Flow Anomaly at Mars

A. Yu. Shestakov[1] and S. D. Shuvalov[1]

[1]Space Research Institute of the Russian Academy of Sciences.

Corresponding author: Artyom Shestakov (sartiom1@yandex.ru)

Key Points:

- O^+ and O_2^+ ions of planetary origin accelerated in a Hot Flot Anomaly are for the first time reported to be observed at Mars
- Ions are accelerated to more than 30 keV at the trailing edge and to ~10 keV on the leading edge of the event
- The ratio of O_2^+ to O^+ maximum energy is consistent with the 1st order Fermi acceleration mechanism

Abstract

Previous observation of a single hot flow anomaly (HFA) at Earth by MMS mission reported solar wind protons effective acceleration inside these structures to nearly 1 MeV under certain conditions via first-order Fermi acceleration process. Current study focuses on the analysis of a single HFA registered at Mars by MAVEN spacecraft. The event is characterized by the presence of accelerated O^+ and O_2^+ ions of planetary origin on both sides from the current sheet associated with the event. Ions with energies up to ~10 keV are detected before the current sheet crossing, and over 30 keV after the current sheet crossing. We report that the relationship between the ion mass and the maximum energy to which acceleration occurs is consistent with the above-mentioned Fermi acceleration process. We hypothetize that effective planetary ions acceleration in HFAs is possible only at unmagnetized planets due to closer bow shock stand-off distance.

Plain Language Summary

Hot flow anomalies (HFAs) are among the largest known types of non-stationary transient events that are formed when a bow shock of a planet encounters a tangential discontinuity (TD) in the interplanetary magnetic field (IMF) of the solar wind that sweeps across the front of the shock, under certain conditions solar wind particles are reflected from the shock to be channeled upstream along the discontinuity. A shock wave is often formed on the upstream edge of a HFA. As this shock sweeps across the plantetary bow shock, these two shocks may converge relative to each other resulting in acceleration of particles that are trapped between them, which is known as the 1st order Fermi acceleration mechanism. Previously, observations of solar wind protons accelerated via this mechanism have been reported in the terrestrial HFA, however, at Mars, much closer bow shock stand-off distance enables for the ionospheric ions to reach the bow shock of the planet when it undergoes significant disturbancies as a result of TD crossing. In this work we report, for the first time, direct observations of planetary oxygen ions acceleration inside a HFA at Mars by The Mars Atmosphere and Volatile Evolution Mission spacecraft.

1 Introduction

Hot flow anomalies (HFAs, Schwartz et al., 1985), along with foreshock bubbles (Turner et al., 2013), are the largest known types of transient events formed at planetary bow shocks. HFAs are formed when a discontinuity in the interplanetary magnetic field (IMF) travelling from the Sun with the solar wind flow meets the bow shock of a planet under certain magnetic field orientations and sweeps across it slowly enough to give time for plasma instabilities to develop. If the motional electric field $\boldsymbol{E} = -1/c\, \boldsymbol{V_{SW}} \times \boldsymbol{B_{IMF}}$ (where c is the speed of light, $\boldsymbol{V_{SW}}$ is the velocity of the solar wind flow, and $\boldsymbol{B_{IMF}}$ is the local IMF vector) is directed towards the discontinuity at its both sides, solar wind particles reflected from the bow shock are channeled in the upstream direction along the discontinuity. Subsequent interaction of these particles with the incident solar wind flow often results in formation of new fast magnetosonic shock on the upstream edge of HFA (Thomsen et al., 1988, Fuselier et al., 1987). The interior of HFA (sometimes referred to as "core") is characterized by low magnetic field magnitude, increased ion temperature and reduced ion number density relative to the solar wind, which is surrounded by compression regions with stronger magnetic field and increased ion concentration. Inside a HFA core, solar wind becomes decelearated and strongly deflected (see, e.g., Liu et al., 2016).

The universality of HFA phenomena is proven by their numerous in-situ observations at the most of the planets in the Solar System: Mercury (Uritsky et al., 2014), Venus (Slavin et al., 2009), Earth (Schwartz et al., 1985), Mars (preliminary observations were reported by Øieroset et al., 2001, and then confidently confirmed by Collinson et al., 2015), Jupiter (Valek et al., 2017), Saturn (Masters et al., 2008, 2009). This widespread occurrence of HFAs in heliosphere at different bow shock sizes varying by several orders of magnitude implies that similar processes may occur at much bigger scales, such as stellar or even galactic shocks, having an impact on the medium underlying the shock surface and being responsible for processes like particle accelerations at astrophysical scales.

Since there often is a shock wave in the upstream edge of HFA which moves with the discontinuity in IMF, inder certain orientation of the discontinuity relative to the bow shock a combination of two converging shock waves can be formed, separated by HFA's core carrying a weak magnetic field. In such configuration, population of charged particles become trapped between two shocks, reflecting at their fronts due to increased magnetic field and smaller gyroradius, and gaining energy at each bounce. The acceleration process continues until the particle's gyroradius becomes large enough to pass through either of the shocks. This process is known as the 1st order Fermi acceleration (Fermi, 1949), and there are recent reports observing accelerated electrons (Liu et al., 2017) and solar wind protons (Turner et al., 2018) via this process at terrestrial foreshock transients.

As HFAs and foreshock transients in general are large-scale events in terms of sizes of planets and their bow shocks, they have an impact on magnetosphere and ionosphere. Thus, acoording to estimates given in Collinson et al., 2012, 2015, a single HFA caused the rise of ionosphere below it to ~70 km at Mars and to ~210 km at Venus due to the decrease of solar wind dynamic pressure on the bow shock in the vicinity of HFA. There are also reports about magenospheric and ionospheric responses to terrestrial foreshock transients (Shen et al., 2018; Wang et al., 2018). It can be assumed that such responses can be even more significant at planets without intrinsic magnetic field as their plasma systems are more compact. Thus, the magnetosheath-ionosphere disturbancies triggered by the passing of a transient event in front of the unmagnetized planet's bow shock may potentially enable for the ionospheric particles to reach the bow shock.

In this paper we report, for the first time, evidence of effective planetary ions acceleration inside a HFA. The analyzed event is chosen from the list of 19 HFAs registered at Mars from the previous research by Shuvalov et al., 2019. No other events from the list exhibit features relaeted to heavy ions acceleration, implying the presence of a number of conditions that must be fulfilled in order for such process to occur and be registered. We hypothetize that effective acceleration of ions of planetary origin in HFAs (or probably other foreshock transients) can happen only at unmagnetized planets, given their closer bow shock stand-off distance to the ionosphere.

The structure of the paper is the following: information aboult the instruments and data products used is presented in section 2; section 3 contains the observation of the event and description of its main features; we discuss the mechanism and causes of the observed acceleration process in section 4; finally, the conclusions are given in section 5.

2 Instrumentation and data

In this research we use data obtained by the Mars Atmosphere and Volatile Evolution spacecraft (MAVEN, Jakosky et al., 2015). Launched in November 2013, it arrived at Mars in September 2014 and was inserted into orbit with ~75° inclination, periapsis ~150 km, apoapsis ~6200 km and orbital period of ~4.5 hours, covering ionospheric, tail, sheath and solar wind regions of the Martian plasma envelope. The data presented in the paper are from Supra-Thermal And Thermal Ion Composition (STATIC), Solar Wind Ion Analyzer (SWIA) ion spectrometers, Solar Wind Electron Analyzer (SWEA) electron spectrometer and magnetometer MAG from from the particles and fields package onboard the spacecraft.

The STATIC instrument (McFadden et al., 2015) mounted on the Actuated Payload Platform is used to study characteristics of different ion species at solar wind-Mars interaction. The instrument consists of a toroidal top hat electrostatic spectrometer with an electrostatic deflector at the entrance providing 360°×90° field of view (FOV) combined with a time-of-flight velocity analyzer resolving the major ion species (H^+, He^+, O^+, O_2^+). It measures energy spectra of ions with different (m/q) in the range of 0.1 eV-30 keV with minimum cadence of 4 seconds and

~15% energy resolution dE/E. The measurements allow a retrieval of the velocity distribution functions and their moments (density, velocity, temperature). STATIC Level 2 d1 data product (Version 2, Revision 0) was used for investigating ions of different species. This dataset contains differential energy fluxes for ions over 32 energy steps, 4 polar and 16 azimuth angles for 8 mass bins. The measurement cadence for the time intervals presented in the paper is 16 seconds. At high count rates some proton data can be wrongly registered as ions of bigger masses due to incorrect identification of start/stop signals of the time-of flight scheme. In order to diminish this effect, we applied a special procedure for O^+ and O_2^+ data, in which 8% of protons differential energy flux was subtracted from oxygen ion data for the same energy and angular bins.

SWIA (Halekas et al. 2015) is also a top-hat ion analyzer with FOV similar to that of STATIC. It does not resolve ion species, however, being mounted on the solar array panel, its orientation is different and chosen in a way that its FOV could continuously observe the direction to the Sun. The energy range of the instrument is from 5 eV to 25 keV per ion charge, energy resolution dE/E ~ 10%. We utilize SWIA onboard survey spectra data bundle (Version 1, Revision 1) which provides ion differential energy fluxes for 48 energy steps, and SWIA key parameters data bundle (Version 18, Revision 3) for obtaining ion number density and bulk velocity derived from the instrument's measurements. The data cadences for these data bundles during the analyzed time interval are 4 and 8 seconds, respectively.

SWEA (Mitchell et al., 2016) is a top-hat electron analyzer with energy range from 5 eV to 4.6 keV, FOV 360°×120° and energy resolution dE/E ~ 17%. We use SWEA survey rate omni-directional electron energy spectra data collection (Version 4, Revision 1) containing differential energy fluxes of electrons for 64 energy steps with time cadence of 4 seconds for the time interval presented in the paper.

MAG (Connereney et al., 2015a, 2015b) is a 3-component magnetometer providing data in 60000 nT dynamic dange with 0.05 nT resolution and 32 Hz time cadence. We use MAG Level 2 data bundle (Version 1, Revision 2) in current research.

3 Observations

The reported event was registered at 19 July 2015, roughly within time interval of 19:25:00 – 19:27:40 UT (see figure 1). During the interval of observations the SC was located at about (1.18, 1.74, 1.77) R_M (where R_M is the radius of Mars) of Martian solar orbital coordinate system

(MSO). In this reference system x-axis is directed toward the Sun, y-axis is backward along the tangent of the orbital plane of Mars, and z-axis completes the right-handed system pointing out of the plane of the Martian ecliptic. This point of observations is located upstream of the bowshock. Main details of the system configuration are listed in table 1.

Approximately at 19:20:00 UT, 5 minutes pror to the HFA registration, both SWIA and STATIC instruments start registering narrowly directed monoenergetic beam of ~10 keV O_2^+ ions and ~6 keV O^+ ions. The energies of these ion populations remains unchanged until 19:25:00 UT, when magnetic field magnitude experiences a sudden drop from ~2.5 nT in the ambient solar wind to ~0.5 nT, indicating spacecraft entrance inside the core of HFA. Simultaneously, ion number density starts dropping from 2.5 cm^{-3} to nearly zero at ~19:26:40, STATIC starts to observe population of hot H^+ ions, which are also features of HFA core, and energies of detected heavy ions start gradually decresing. Another milestone in the timeline of event registration is 19:26:00 UT, when magnetic field experiences a turn at ~160°, indicating the intersection of HFA-related discontinuity, or current sheet (CS), by the spacecraft. This turn is accompanied by the increase of magnetic field magnitude to ~7.9 nT, which then returns to its previous value of ~0.5 nT within ~15 seconds. Also, a population of hot electrons is observed by SWIA during CS crossing (panel (e) in figure 1). Approximately 40 seconds later, the spacecraft enters the HFA upstream compression region, in which magnetic field magnitude has two spikes up to ~16 nT at 19:27:00 UT and 19:27:30 UT, solar wind becomes decelerated from ~510 km/s to ~320 km/s and ion number density begins to increase, peaking at 3.3 cm^{-3} and then returning to ~2.8 cm^{-3} in the solar wind. Hot electron populations are observed simultaneously with magnetic field magnitude peaks in the compression region.

Starting at 19:27:00 UT, SWIA (panel (a) in figure 1) starts to register another highly accelerated ion population with energy of ~10 keV which quickly increases in time and quits the energy range that the instrument is capable to detect at ~19:27:35 UT. The same population is registered by STATIC (panels (c) and (d) in figure 1) which keeps detecting it for a little bit longer time (nearly 19:28:00 UT) due to its higher maximum energy registration limit. According to STATIC measurements, this populations consists of O^+ and O_2^+ ions with the dominant component of O_2^+ ions.

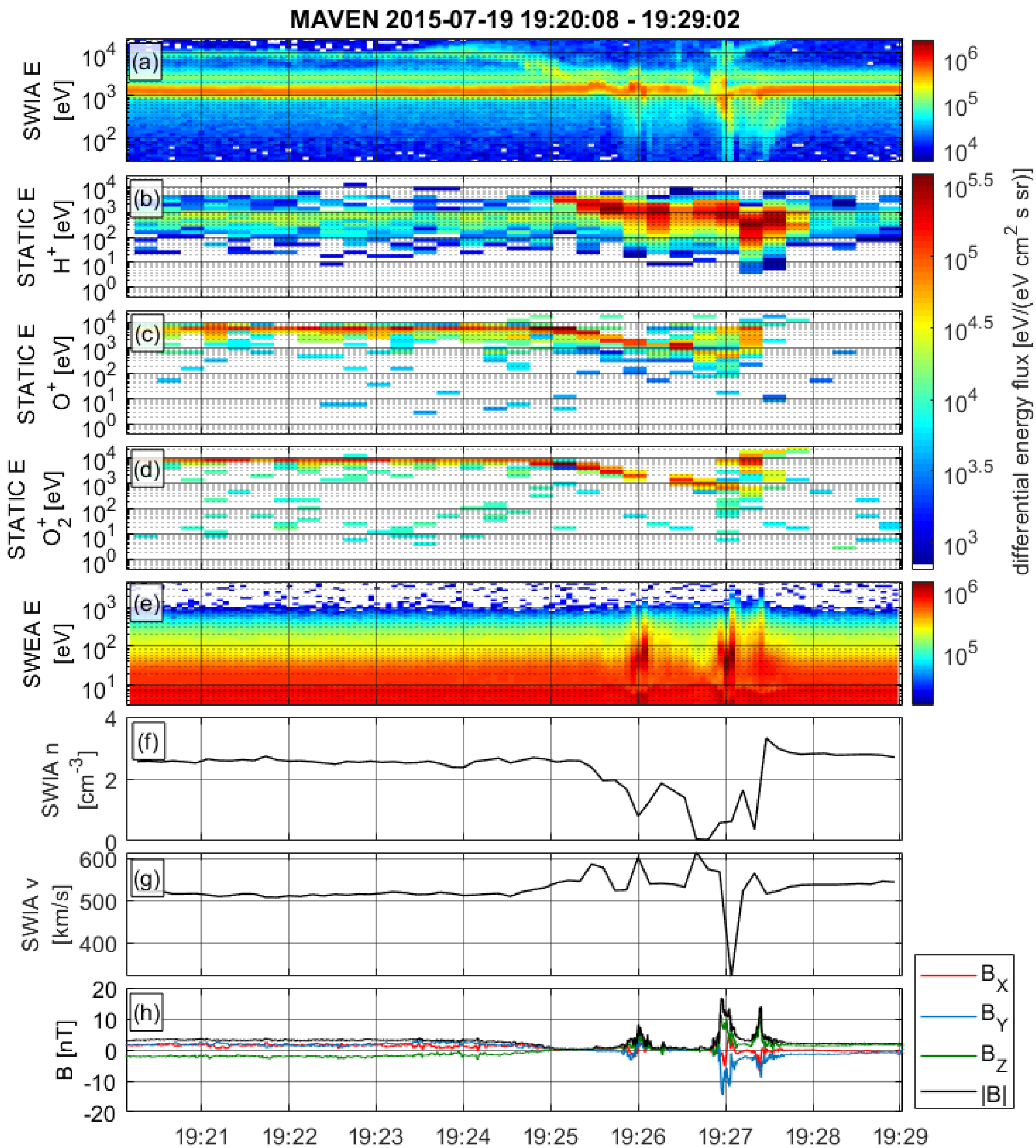

Figure 1. A HFA event with accelerated planetary ions. (a) – ion energy-time spectrogram measured by SWIA (all ions), (b)-(d) – H^+, O^+, O_2^+ ion energy-time spectrograms measured by STATIC, (e) – electron energy-time spectrogram measured by SWEA, (f) and (g) – ion density and bulk velocity derived from SWIA, (h) – three components and magnetic field magnitude in MSO coordinate system.

Table 1. Main characteristics of the observed HFA.

Parameter	***Value***
Location of HFA (MSO, R_M)	(1.18, 1.74, 1.77)
Average V_{SW}	540 km/s
Magnetic field rotation	~161°
θ_{Bn} before/after the event	66°/85° (quasi-⊥ BS)
CS normal (MSO)	(-0.38, 0.67, 0.64)
CS velocity	202 km/s
$n_{cs} - V_{SW}$ angle	~112°
Distance to the BS, R_M	0.72

4 Analysis

The orientation of the HFA-related CS was estimated in the assumption of an infinite planar tangential discontinuity (e.g. it has zero normal magnetic field component), calculating the cross product of magnetic field vector averaged over periods of time 19:23:30–19:24:30 and 19:27:41–19:28:30 UT, during which the spacecraft was in the undisturbed solar wind region prior and after the HFA registration, respectively. The angle between the resulting CS normal with the solar wind is ~112°, which, accroding to the criteria for HFA formation listed in Schwartz et al., 2000, can be considered as big enough to reduce the CS speed relative to the planet and give HFA sufficient time to develop. Despite the relatively high solar wind speed, ~540 km/s, the speed of CS calculated as projection of $\mathbf{V_{SW}}$ to CS normal direction, is only ~202 km/s. The angle θ_{Bn} between magnetic field and the bow shock was calculated at the nearest intersection point between IMF and the bow shock model derived by Trotignon et al., 2006, and shows values 66° and 85° prior and after the event, respectively, which is consistent with quasi-perperndicular bow shock on both sides of the CS. The closest distance from the event to the bow shock along the IMF line is ~0.72 R_M which is close enough for a HFA registration at Mars.

In order to trace the accelerated heavy ions seen before the CS crossing, these populations have been selected from angular distribution function measured by STATIC as a result of applying a mask to its angular bins. Ion bulk velocity vectors have been calculated as 1st moment of resulting distribution function and averaged over a period of time 19:20:00-19:25:00 UT. The directions of these vectors, combined with the orientation of the CS and the MAVEN position relative to Mars and its bow shock, is presented in figure 2 in 3 projections of MSO coordinates. It is seen that O^+ and O_2^+ ion velocities are directed roughly towards CS propagation speed which is a strong evidence that these particles are HFA-related.

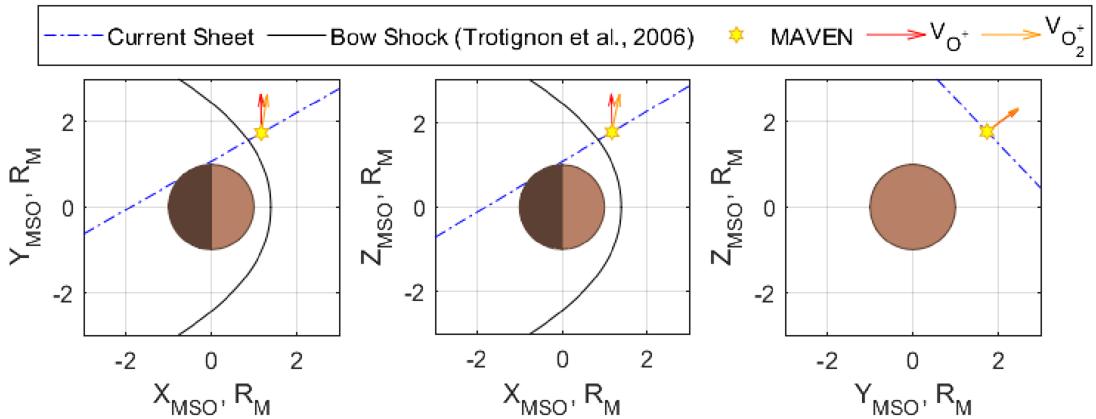

Figure 2. Three projections of HFA registration position in MSO coordinates with orientation of the current sheet related to the event, idealized bow shock position derived from Trotignon et al., 2006 and velocity vectors of accelerated O^+ and O_2^+ ions detected prior the event registration.

Following Turner et al., 2018, we check if maximum energy of accelerated O^+ and O_2^+ ions satisfy condition for the 1st order Fermi acceleration $\frac{E_{max}{}^2}{mq} = const$. According to it, these energies must differ from each other by $\sqrt{2}$ times. Given that the maximum energy of O^+ ions detected at the leading edge of HFA is ~6.8 keV (see figure 3), the predicted maximum energy of O_2^+ ions must be ~9.6 keV. The actual measured maximum energy of these ions is ~9.75 keV which lies well within the STATIC energy resolution error (15%) of the predicted value.

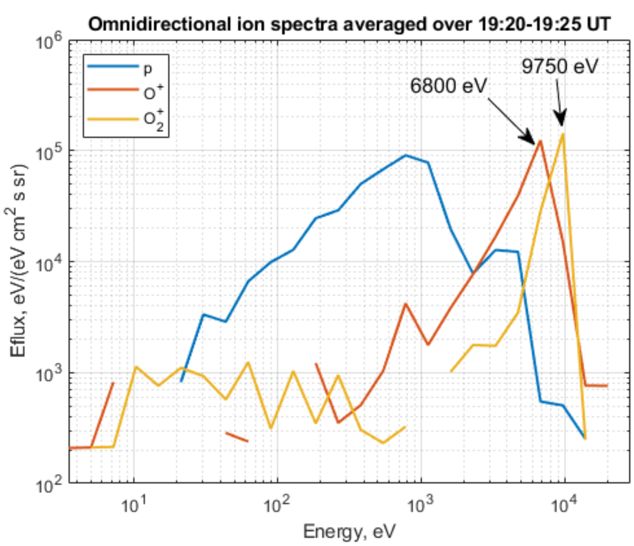

Figure 3. Omnidirectional ion energy spectra for H^+, O^+ and O_2^+ ions averaged over 19:20:00-19:25:00 UT derived from STATIC measurements.

5 Conclusion

This paper reports observation of heavy ions acceleration in a HFA at Mars to energies up to ~10 keV on the leading edge and up to more than 30 keV at the trailing edge of the event. The ratio of O_2^+ to O^+ maximum acceleration energy on the leading side of HFA is consistent with the 1st order Fermi acceleration mechanism. Unlike previously reported similar acceleration mechanism in terrestrial HFA (Turner et al., 2018), the species of accelerated particles are predominantly heavy ions of ionospheric origin, which, apparently, is the feature of HFAs at unmagnetized planets. Being capable of accelerating particles to velocities, exceeding the escape velocity at Mars (~2 eV for O^+ and ~4 eV for O_2^+ ions), this mechanism reveals another Martian atmospheric loss channel.

Acknowledgments

The research is sponsored by the Russian Science Foundation (RSF) grant 21–42–04404. The authors express gratitude to MAVEN team for the research data.

Open Research

The MAVEN data used in this study can be accessed from the NASA Planetary Data System via link below (see directories for STATIC, SWIA, SWEA and MAG instruments) (https://pds-ppi.igpp.ucla.edu/search/?t=Mars&sc=MAVEN&facet=SPACECRAFT_NAME&depth=1)

References

Collinson, G.A., et al., 2012. Hot flow anomalies at Venus. J. Geophys. Res. 117, A04204. https://doi.org/10.1029/2011JA017277.

Collinson, G., et al., 2015. A hot flow anomaly at Mars. Geophys. Res. Lett. 42, 9121–9127. https://doi.org/10.1002/2015GL065079.

Connerney, J.E.P., Espley, J.R., Di Braccio, G.A., Gruesbeck, J.R., Oliversen, R.J., Mitchell, D.L., et al., 2015a. First results of the MAVEN magnetic field investigation. Geophys. Res. Lett. 42, 8819–8827. https://doi.org/10.1002/2015GL065366.

Connerney, J.E.P., Espley, J.R., Lawton, P., Murphy, S., Odom, J., Oliversen, R., Sheppard, D., 2015b. The MAVEN magnetic field investigation. Space Sci. Rev. 195 (1–4), 257–291. https://doi.org/10.1007/s11214-015-0169-4.

Fermi, E. On the origin of cosmic radiation. Phys. Rev. 75, 1169–1174 (1949) https://doi.org/10.1103/PhysRev.75.1169.

Fuselier, S. A. et al. Fast shocks at the edges of hot diamagnetic cavities upstream from the Earth's bow shock. J. Geophys. Res. 92, 3187–3194 (1987) https://doi.org/10.1029/JA092iA04p03187.

Halekas, J.S., Taylor, E.R., Dalton, G. et al. The Solar Wind Ion Analyzer for MAVEN. Space Sci Rev 195, 125–151 (2015). https://doi.org/10.1007/s11214-013-0029-z

Jakosky, B. M., Lin, R. P., Grebowsky, J. M., Luhmann, J. G., Mitchell, D. F., Beutelschies, G., et al. (2015). The Mars Atmosphere and Volatile Evolution (MAVEN) mission. Space Science Reviews, 195, 3–48. https://doi.org/10.1007/s11214-015-0139-x

Liu, T. Z., Turner, D. L., Angelopoulos, V. & Omidi, N. Multipoint observations of the structure and evolution of foreshock bubbles and their relation to hot flow anomalies. J. Geophys. Res. 121, 5489–5509 (2016) https://doi.org/10.1002/2016JA022461.

Liu, T. Z. et al. Fermi acceleration of electrons inside foreshock transient cores. J. Geophys. Res. 122, 9248–9263 (2017) https://doi.org/10.1002/2017JA024480.

Masters, A., et al., 2008. Cassini encounters with hot flow anomaly-like phenomena at Saturn's bow shock. Geophys. Res. Lett. 35, L02202. https://doi.org/10.1029/2007GL032371.

Masters, A., et al., 2009. Hot flow anomalies at Saturn's bow shock. J. Geophys. Res. 114, a08217. https://doi.org/10.1029/2009JA014112.

McFadden, J.P., Kortmann, O., Curtis, D., Dalton, G., Johnson, G., Abiad, R., et al., 2015. MAVEN SupraThermal and thermal ion composition (STATIC) instrument. Space Sci. Rev. 195 (1–4), 199–256. https://doi.org/10.1007/s11214-015-0175-6.

Mitchell, D.L., Mazelle, C., Sauvaud, JA. et al. The MAVEN Solar Wind Electron Analyzer. Space Sci Rev 200, 495–528 (2016). https://doi.org/10.1007/s11214-015-0232-1

Øieroset, M., Mitchell, D.L., Phan, T.D., Lin, R.P., Acu~na, M.H., 2001. Hot diamagnetic cavities upstream of the Martian bow shock. Geophys. Res. Lett. 28, 887–890. https://doi.org/10.1029/2000GL012289

Schwartz, S.J., Chaloner, C.P., Hall, D.S., Christiansen, P.J., Johnstones, A.D., 1985. An active current sheet in the solar wind ISSN0028–0836. Nature 318, 269–271. https://doi.org/10.1038/318269a0

Schwartz, S. J., G. Paschmann, N. Sckopke, T. M. Bauer, M. Dunlop, A. N. Fazakerley, and M. F. Thomsen (2000), Conditions for the formation of hot flow anomalies at Earth's bow shock, J. Geophys. Res., 105, 12,639–12,650.

Shen, X.-C., Shi, Q., Wang, B., Zhang, H., Hudson, M. K., Nishimura, Y., et al. (2018). Dayside magnetospheric and ionospheric responses to a foreshock transient on 25 June 2008: 1. FLR observed by satellite and ground-based magnetometers. Journal of Geophysical Research: Space Physics, 123, 6335–6346. https://doi.org/10.1029/2018JA025349

Shuvalov S.D., Ermakov V.N., Zorina V.O., Kim K.I., Propagation properties of Hot Flow Anomalies at Mars: MAVEN observations, Planetary and Space Science, Volume 179, 2019, 104717, ISSN 0032-0633, https://doi.org/10.1016/j.pss.2019.104717.

Slavin, J.A., et al., 2009. MESSENGER and Venus Express observations of the solar wind interaction with Venus. Geophys. Res. Lett. 36, L09106. https://doi.org/10.1029/2009GL037876.

Thomsen, M. F. et al. On the origin of hot diamagnetic cavities near the Earth's bow shock. J. Geophys. Res. 93, 11311–11325 (1988)

Trotignon, J.G., Mazelle, C., Bertucci, C., Acuna, M.H., 2006. Martian shock and magnetic pile-up boundary positions and shapes determined from the Phobos 2 and Mars Global Surveyor data sets. Planet. Space Sci. 54, 357–369. https://doi.org/10.1016/j.pss.2006.01.003.

Turner, D.L., Omidi, N., Sibeck, D.G., and Angelopoulos, V., First observations of foreshock bubbles upstream of Earth's bow shock: Characteristics and comparisons to HFAs, J. Geophys. Res.: Space Phys., 2013, vol. 118, pp. 1552–1570. https://doi.org/10.1002/jgra.50198

Turner, D.L., Wilson, L.B., Liu, T.Z., Cohen, I.J., Schwartz, S.J., Osmane, A., Fennell, J.F., Clemmons, J.H., Blake, J.B., Westlake, J., Mauk, B.H., Jaynes, A.N., Leonard, T., Baker, D.N., Strangeway, R.J., Russell, C.T., Gershman, D.J., Avanov, L., Giles, B.L., Torbert, R.B., Broll, J., Gomez, R.G., Fuselier, S.A., Burch, J.L., 2018. Autogenous and efficient acceleration of energetic ions upstream of Earth's bow shock. Nature 561, 206–2010. https://doi.org/10.1038/s41586-018-0472-9.

Uritsky, V.M., et al., 2014. Active current sheets and candidate hot flow anomalies upstream of Mercury's bow shock. J. Geophys. Res. A Space Phys. 119, 853–876. https://doi.org/10.1002/2013JA019052.

Valek, P.W., et al., 2017. Hot flow anomaly observed at Jupiter's bow shock. Geophys. Res. Lett. 44, 8107–8112. https://doi.org/10.1002/2017GL073175.

Wang, B., Nishimura, Y., Hietala, H., Shen, X.-C., Shi, Q., Zhang, H., et al. (2018). Dayside magnetospheric and ionospheric responses to a foreshock transient on 25 June 2008: 2. 2-D evolution based on dayside auroral imaging. Journal of Geophysical Research: Space Physics, 123, 6347–6359. https://doi.org/10.1029/2017JA024846

Figure 1.

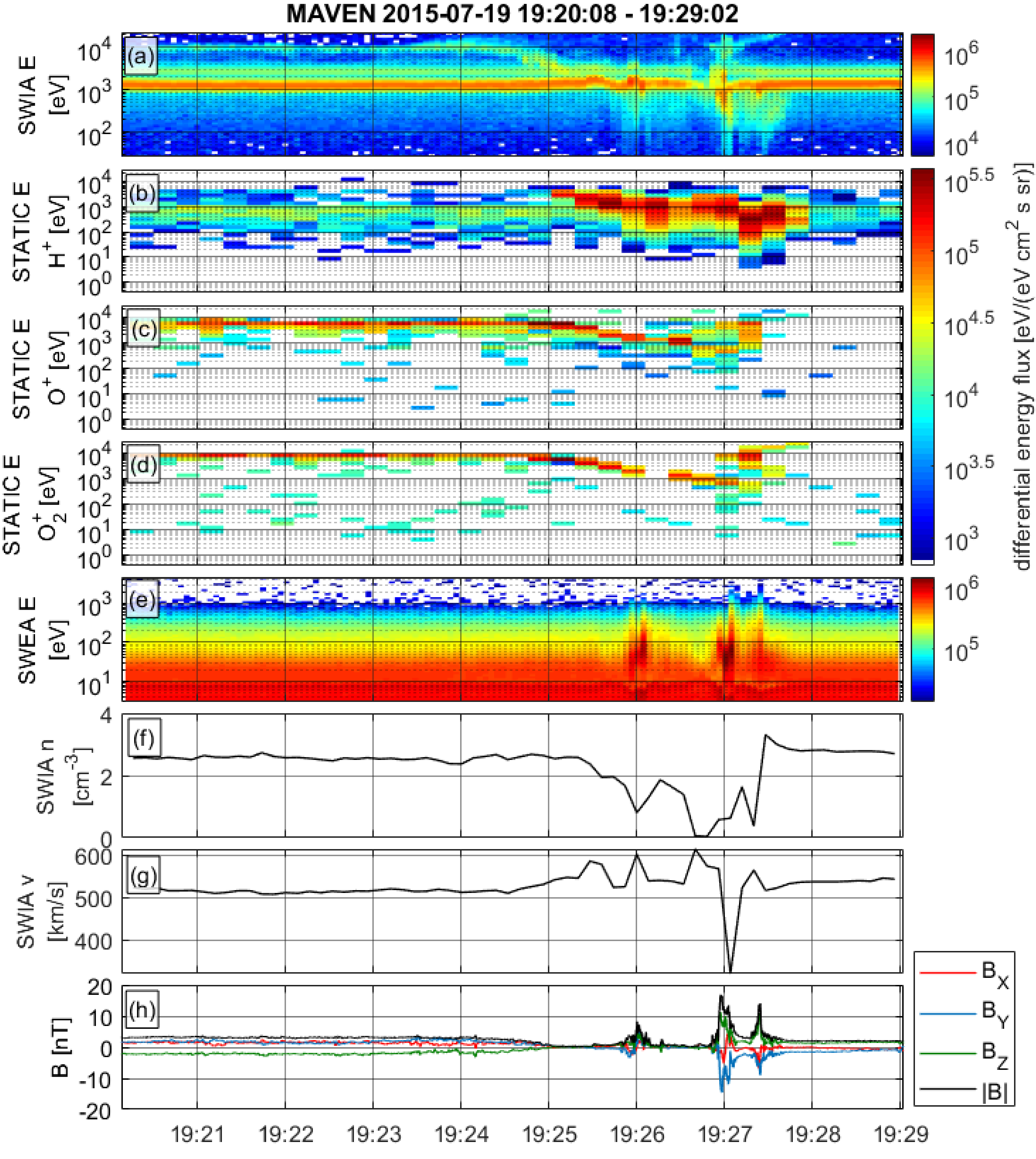

MAVEN 2015-07-19 19:20:08 - 19:29:02
(a)
SWIA E [eV]
(b)
STATIC E H+ [eV]
(c)
STATIC E O+ [eV]
(d)
STATIC E O2+ [eV]
(e)
SWEA E [eV]
(f)
SWIA n [cm-3]
(g)
SWIA v [km/s]
(h)
B [nT]
differential energy flux [eV/(eV cm2 s sr)]
BX
BY
BZ
|B|
19:21
19:22
19:23
19:24
19:25
19:26
19:27
19:28
19:29

Figure 2.

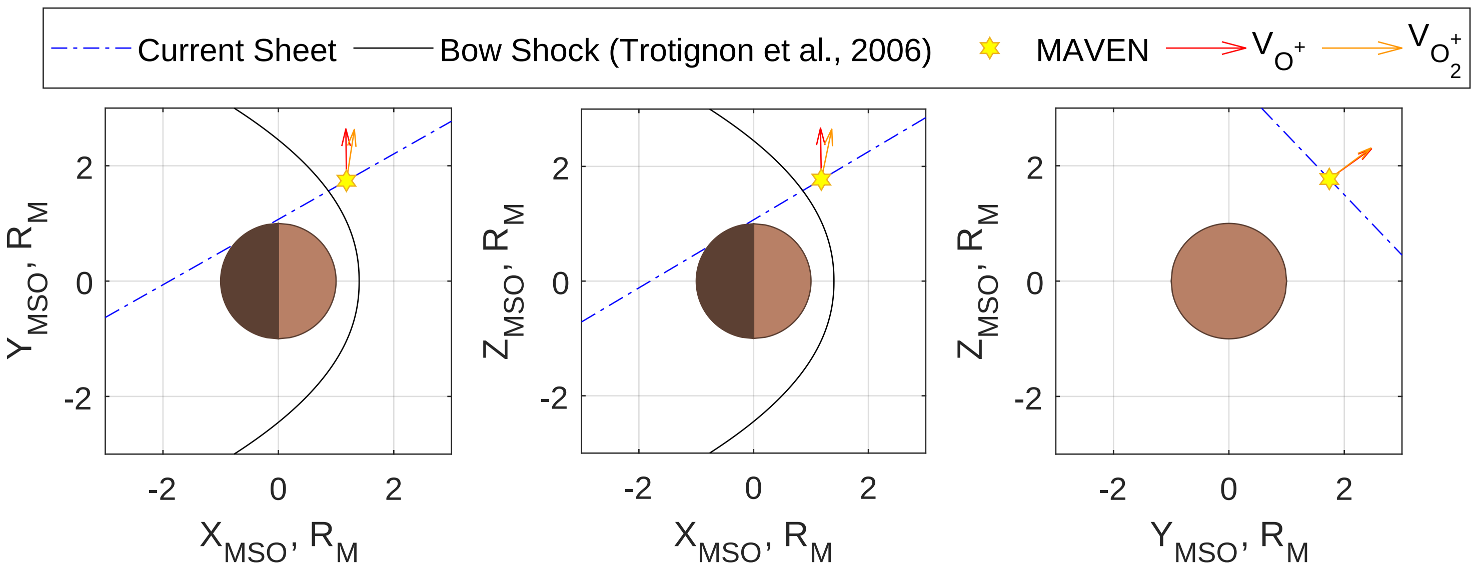
Current Sheet
Bow Shock (Trotignon et al., 2006)
MAVEN
V_{O^+}
$V_{O_2^+}$
Y_{MSO}, R_M
X_{MSO}, R_M
Z_{MSO}, R_M
X_{MSO}, R_M
Z_{MSO}, R_M
Y_{MSO}, R_M

Figure 3.

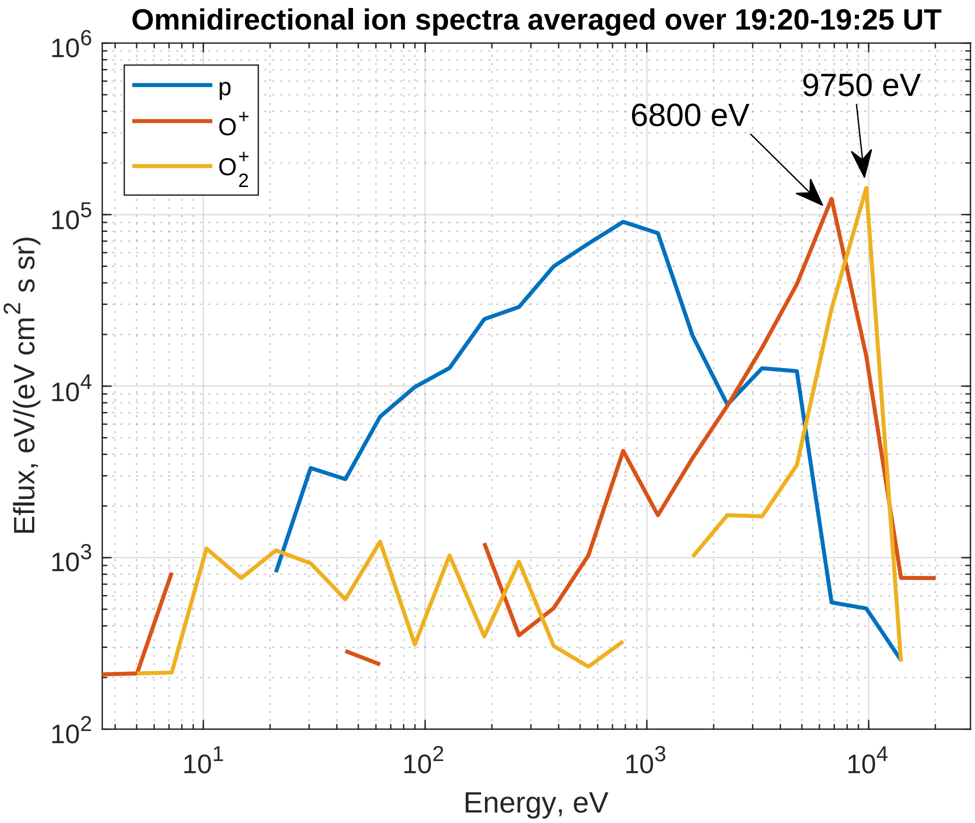

Omnidirectional ion spectra averaged over 19:20-19:25 UT
p
O+
O2+
6800 eV
9750 eV
Eflux, eV/(eV cm2 s sr)
Energy, eV
10^2
10^3
10^4
10^5
10^6
10^1
10^2
10^3
10^4